RAPID COMMUNICATION | OCTOBER 08 2024

No more gap-shifting: Stochastic many-body-theory based TDHF for accurate theory of polymethine cyanine dyes

Nadine C. Bradbury ; Barry Y. Li ; Tucker Allen ; Justin R. Caram ; Daniel Neuhauser

J. Chem. Phys. 161, 141101 (2024)
https://doi.org/10.1063/5.0223783
CHORUS

The Journal of Chemical Physics COMMUNICATION pubs.aip.org/aip/jcp

No more gap-shifting: Stochastic many-body-theory based TDHF for accurate theory of polymethine cyanine dyes

Cite as: J. Chem. Phys. 161, 141101 (2024); doi: 10.1063/5.0223783
Submitted: 17 June 2024 • Accepted: 15 August 2024 •
Published Online: 8 October 2024

Nadine C. Bradbury,[a] Barry Y. Li, Tucker Allen, Justin R. Caram,[b] and Daniel Neuhauser[c]

AFFILIATIONS

Department of Chemistry and Biochemistry, University of California, Los Angeles, California 90095, USA

[a]Author to whom correspondence should be addressed: nadinebradbury@ucla.edu
[b]jcaram@chem.ucla.edu
[c]dxn@ucla.edu

ABSTRACT

We introduce an individually fitted screened-exchange interaction for the time-dependent Hartree–Fock (TDHF) method and show that it resolves the missing binding energies in polymethine organic dye molecules compared to time-dependent density functional theory (TDDFT). The interaction kernel, which can be thought of as a dielectric function, is generated by stochastic fitting to the screened-Coulomb interaction of many-body perturbation theory (MBPT), specific to each system. We test our method on the flavylium and indocyanine green dye families with a modifiable length of the polymethine bridge, leading to excitations ranging from visible to short-wave infrared. Our approach validates earlier observations on the importance of inclusion of medium range exchange for the exciton binding energy. Our resulting method, TDHF@v_W, also achieves a mean absolute error on a par with MBPT at a computational cost on a par with local-functional TDDFT.

In 1948, Kuhn showed that the optical transitions of organic cyanine dyes could reasonably be described by the "particle in a box" (PIB) free electron gas model.[1] Such a simplistic quantum theory works astoundingly well for these systems. In fact, since then, it has been widely shown that the commonly used modern quantum chemistry methods for optical spectroscopy, time-dependent Hartree–Fock (TDHF), and all varieties of time-dependent density functional theory (TDDFT) have much lower accuracy, often up to 1.0 eV error in transition energy.[2] This is known as the "cyanine problem" of TDDFT. The PIB model succeeds because the PIB orbitals do resemble the frontier molecular orbitals (MOs) of cyanine dyes, with both the highest-occupied π MO (HOMO) and the lowest-unoccupied π^* MO (LUMO) fully delocalized over the large polymethine backbone. With modern quantum chemistry methods, achieving such full delocalization is challenging without a full long-range exchange interaction, rendering local density functional theory (DFT) methods poorly suited. The complete exchange interaction of HF may yield accurate-looking molecular orbitals, but correct excitation energies require a detailed balance of long-range charge transfer and local valence excitations. Indeed, the amount of HOMO to LUMO wavefunction overlap and the predicted excitation energy have been shown to be directly proportional to the medium range component of the exchange in a chosen hybrid density functional.[3] Given such high dependency on functional choice in these systems, it is common to apply an arbitrary rigid energy shift when compared to experimental spectra.

To provide an *ab initio* approach to correct excitation energies, many-body perturbation theory (MBPT) methods, such as the *GW*+Bethe–Salpeter Equation (BSE) approach, have been shown to achieve much better accuracy (~0.1 eV). The multideterminantal nature of cyanine dyes is indeed important. Boulanger *et al.* highlighted that BSE, despite being built on a monodeterminantal ground state, effectively includes nonlocal correlation effects through the screened Coulomb potential.[4,5] This allows BSE to capture some of the complex multiconfigurational characteristics of excitations that are not properly described with TDDFT methods. The improved accuracy from BSE comes at a high cost, as these methods scale steeply with system size, so they are very expensive to be applied for large molecules with hundreds of electrons as used in biological imaging with very low excitation energies in the near

and short-wave infrared range (NIR: λ = 700–1000 nm and SWIR: λ = 1000–2000 nm).

Recently, we have developed stochastic methodologies that reduce the computational scaling of the BSE, unlocking the study of systems up to several thousands of electrons.[6,7] In these works, we pair an iterative approach to calculate the full optical spectra of the molecule, with a stochastic approach to determine the screened-Coulomb interaction W, the typically expensive part of the BSE.[6] In our most recent work, we use stochastic time-dependent Hartree (TDH) propagation to fit a translationally invariant exchange kernel $v_W(r-r')$, which is custom for each system and has a nearly equivalent effect acting on a pair density as the full screened-Coulomb interaction $W(r,r')$ and similar overall accuracy for the optical gap.[7] We term this individually fitted interaction v_W, and when replacing the full W in BSE with v_W, the resulting equation is a version of TDHF using v_W in the exchange response kernel, henceforth referred to as TDHF@v_W.

Building a modified exchange kernel is the original principle behind the optimally tuned Fock exchange contribution in range-separated hybrid functional methods, where the smoothness and the total amount of long-range exchange are fitted to give accurate ionization potentials by partial charging of the system.[8] However, for many systems, limiting the functional form of the exchange kernel is too strong of an assumption. In fact, the key to the accuracy of the BSE approach is the use of the effective interaction $W(r,r',\omega)$ instead of a prior prescribed exchange interaction. There are multiple ways this could be achieved, and most generally, use the static approximation $W = W(\omega = 0)$. Sharma *et al.* attempted to improve the TDDFT spectra of extended systems by iteratively refining an approximate static *xc* (exchange–correlation) kernel.[9] Their bootstrap approach uses the system's dielectric response within the RPA (random-phase approximation), showing excellent agreement with BSE results at a lower computational cost for periodic systems.[10] The present TDHF@v_W approach aims to reduce computational cost of fitting an *xc* kernel and retain the accuracy of the BSE to address difficult large molecules, such as conjugated polymethine dyes, using an efficient stochastic calculation of the effect of W starting from an accurate hybrid functional. Instead of imposing a specific functional form on the exchange, we directly access the exchange kernel, or dielectric function, at all length scales using stochastic fitting.

While TDHF is less expensive than the full BSE, it can still be considerably costly for larger systems. To reduce the effective scaling, we use a split deterministic-sparse stochastic compression scheme to efficiently calculate and store all the attenuated exchange integrals. As detailed in our previous work, the v_W approach reduces the formal scaling of the effective interaction W from $\sim O(N^4)$ to $\sim O(N^3)$ with respect to the number of electrons by employing stochastic sampling.[17,18] The exchange kernel v_W captures the bulk of the effect of the screened interaction W by evaluating the action of the effective interaction on stochastic orbital pairs. Generally, ~500 stochastic orbital pair density samples are sufficient for convergence, as shown in Fig. S5. This approach is efficient since the number of stochastic samples required to construct v_W does not grow with system size. We study the flavylium (Flav) and indocyanine green (ICG) families of dyes due to their tunable and experimentally well-characterized molecular structures, bulkiness in size, and outstanding impact in the fields of shortwave infrared (SWIR) used for biological imaging.[11,19,20] All the dye geometries are optimized at the PBE0/def2-TZVPP level of theory using the ORCA 5.0 program.[21] We show that a modified exchange kernel, which includes more exchange at "medium-k" than conventional range-separated hybrid functionals, recovers the missing binding energies found in these dye molecules.

The primary object of theoretical interest in this Communication is the translationally invariant screened-Coulomb interaction in the style of MBPT. The theoretical development of the optimization of this interaction is detailed in Ref. 7 and summarized here. The translationally invariant screened potential is a function of the form $v_W(r-r')$ that minimizes the difference from the true static $W(r,r')$ screened potential over all occupied orbital pair densities $(\phi_i\phi_j)$. Instead of sampling all occupied densities to construct each screened exchange kernel, we introduce a set of stochastic pair density samples $\tilde{\beta}(r) = \sum_i (\pm 1)\phi_i(r)$, where $i \le N_{\mathrm{occ}}$. Since we choose $v_W(r-r')$ to be diagonal in momentum space, the optimal form of v_W is extracted as

$$v_W(k) = \frac{\{\beta^*(k)\langle k|W|\beta\rangle\}}{\{|\langle k|\beta\rangle|^2\}}, \tag{1}$$

where $\{\cdots\}$ indicates a statistical average and $\beta(r) \equiv \tilde{\beta}(r)\bar{\tilde{\beta}}(r)$ is a pair density of independent stochastic orbitals.

The crucial ingredient in Eq. (1) is the action of the full many-body W on the random pair density, $\langle k|W|\beta\rangle = W_\beta(k)$. This is obtained as introduced in Refs. 6, 7, and 22 through a stochastic TDH propagation with a source potential derived from $\beta(r)$ and summarized here. In MBPT, $W = v + v\chi v \equiv v + W^{\mathrm{pol}}$ is derived from a static Coulomb interaction and a polarization-mediated interaction component.[23] The action can be written as $W_\beta = q_\beta + W^{\mathrm{pol}}_\beta$ with source potential $q_\beta = \int dr'\beta(r')|r-r'|^{-1}$. The polarization component is generated from a TDH propagation comparing unperturbed and perturbed stochastic orbitals, $\eta'_s = e^{-i\alpha q_\beta(r)}\eta_s(r)$, evolved by

$$i\dot{\eta}'_s(r,t) = (H_0 + u_\beta(r) + \hat{X}_0(t))\eta'_s(r,t), \tag{2}$$

where $u_\beta(r,t) = \int dr'|r-r'|^{-1}(n^\alpha(r',t) - n^{\alpha=0}(r',t))$, made from a stochastic density $n^\alpha(r,t) = 2\{|\eta_s(r,t)|^2\}_s$. Next, the exchange term is completed with stochastic orbitals, as recently developed for GW theory in Ref. 24. Using a hybrid-orbital starting point for this step in MBPT has been shown to improve results substantially.[25]

Another crucial aspect of achieving good results in stochastic propagation for the action is the orthogonality routine, which removes the occupied–occupied contamination in the propagated perturbed molecular orbitals.[7] In particular, approximately every dozen time steps, a projection of the stochastic orbitals is performed to remove this contamination, i.e.,

$$\eta^\alpha_s(t) \to \eta^{\alpha=0}_s(t) + (\boldsymbol{I} - \boldsymbol{P})(\eta^\alpha(t) - \eta^{\alpha=0}(t)), \tag{3}$$

with $\boldsymbol{P}$ being a projection onto all occupied orbitals, followed by a renormalization of η_s.

Finally, the action of W on β is obtained by

$$W_{\beta}^{pol}(r) = \alpha^{-1} \int dt u_{\beta}(r,t) e^{-\gamma^2 t^2}, \tag{4}$$

where $\gamma = 0.1$ a.u. serves as a numerical damping parameter for efficient convergence and the statistical error is sufficiently controlled even when only ten stochastic η orbitals are used.

One can consider that $v_W^{\mathrm{pol}} = v_W - v$ contains information from the dielectric function of the molecule, following the expression $1 + \epsilon^{-1}(k) = v_W^{\mathrm{pol}}(k)/v(k)$, with v the bare non-periodic Coulomb interaction.

Optical electronic absorption spectra for these chosen dyes are then extracted using a TDHF simulation with the fitted v_W made uniquely for each dye molecule. The full technique for this calculation is detailed in Ref. 18, where it is benchmarked to other electronic structure software. For each dye molecule, we use a near-gap hybrid DFT (ngH-DFT) approach at content-addressable memory (CAM)-LDA0 level as a starting point. Therefore, we use hybrid DFT eigenvalues in place of GW-corrected eigenvalues as in a standard GW+BSE calculation.[17] Using a frequency-domain Chebyshev approach, we obtain the TDHF@v_W spectra by propagating all occupied and 400 unoccupied orbitals. We use the previously developed sparse-stochastic compression technique to evaluate the v_W matrix elements with a total of 1000 short stochastic fragments.[7,18] A full analysis of the computational cost of BSE, TDHF@v_W, and TDDFT is included in Ref. 7. TDHF@v_W here requires about 1000 core hours per dye, with a similar run time for the TD-CAM-LDA0. Stochastic BSE requires a factor of 3–5 more time than the TDHF@v_W approach. Deterministic BSE was not performed here due to its high computational cost for systems with ~150 occupied orbitals, but we have earlier verified[7] that stochastic BSE matches deterministic BSE. As shown in our previous work, BSE peaks generally matches TDHF@v_W to within 0.1 eV and has a similar mean absolute error (MAE). For comparison, we include optical gaps for the Flav dye series obtained with the stochastic BSE in Table S1. Further BSE results and detailed comparison will be supplied in a future paper.

Figure 1 presents the principal results of this work for both Flav (a) and ICG (b) families of dyes. The fitted-interaction TDHF@v_W method significantly enhances the accuracy of predicting the optical gap in polymethine dyes, closely aligning with experimental spectra.[11,13–16,26] For the Flav dyes, the consistent relative error observed between dyes with varying lengths of polymethine bridges in both TDDFT and TDHF@v_W suggests that these errors stem from the ground-state computations and the challenges in optimizing large planar molecules, rather than from inconsistency in the binding energy calculations from TDHF@v_W.

Figure 1(b-ii) shows the lowest-energy exciton density of ICG-7 extracted directly from iterative studies,[6,7,27] in which the electron is polarized along heterocycle of the dye, giving the expectant strong transition dipole moment of these molecules. Meanwhile, the hole density is concentrated in the π-bonding orbital of the cyanine backbone and is mostly derived from the HOMO.

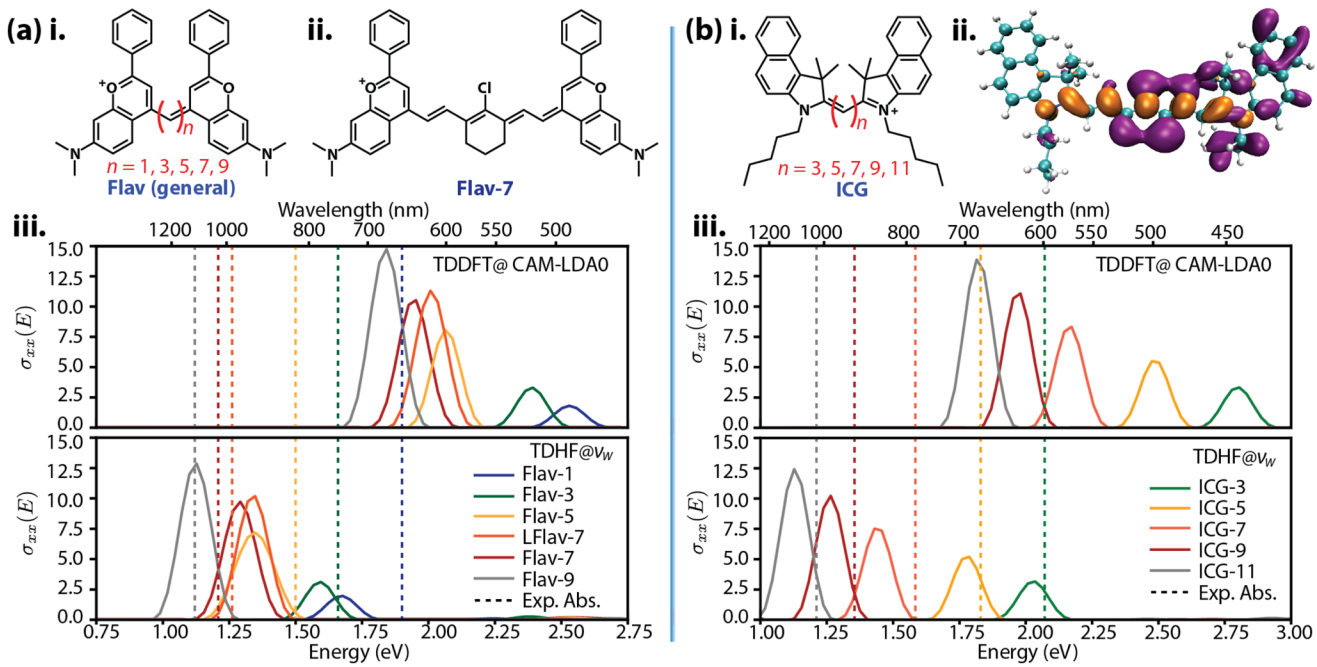

FIG. 1. (a) Lewis structures (i) and (ii) and linear response absorption cross section (iii) for the Flav dye family for TDDFT@CAM-LDA0 and TDHF@v_W. Experimental $\lambda_{\max}$ in water solution (dashed vertical lines) for the Flav dyes are extracted from Ref. 11. LFlav-7 stands for "linear Flav-7," and it does not have a ring structure in the middle of the polymethine bridge (unlike the typical Flav-7). (b) Lewis structure (i), ICG-7 exciton density showing the electron (purple) and hole (orange) (ii), and linear response absorption cross section (iii) for the ICG dye family using both TDDFT@CAM-LDA0[12] and TDHF@v_W. Experimental $\lambda_{\max}$ in water solution values for the ICG dyes are extracted from Refs. 13–16.

Figures 2(a) and 2(b) show the fitted polarization potential, v_W^{pol}, for both dye families, noting their striking similarity. In (c), the ratio between v_W^{pol} and the bare non-periodic Coulomb interaction $v(k)$ can be thought of as the fraction of exact exchange *removed due to screening* in k-space, recalling that the bare Coulomb interaction is $4\pi/k^2$. To facilitate comparison, we also show the amount of exchange removed by screening with the originally optimized parameters of the CAM-LDA0 functional ($\alpha = 0.19$, $\beta = 0.46$, $\mu = 0.33$), and BNL functional with $\gamma = 0.15$.[8,12,28,29] It is shown in Fig. 2(c) that the CAM-LDA0 functional leads to over-screening at medium range with $\epsilon^{-1}(k)$ showing a leveling off to α at medium- and high-k. The $\epsilon^{-1}(k)$ derived from $v_W^{\mathrm{pol}}(k)$ is able to capture the unique behavior of the exchange kernel at medium-range.

The fact that the v_W functions for all dyes largely overlap each other shows that the amount of screening (and thereby polarizability) is similar between dyes of varying polymethine bridge length and family (choice of heterocycle). This notably brings hope for a universal screened exchange kernel for use in highly delocalized organic systems that can accurately describe medium-range behavior. Future studies will determine whether such a universal potential exists.

In (d) and (e), we show the fitted $v_W(k)$ along the cardinal k-paths in k-space and the corresponding $rv_W(r)$ values in real space, once again showing the fraction of removed exchange due to screening. One observes the nearly isotropic behavior of v_W at high-k (short range) but notable deviations at low-k (long-range). This makes sense as polymethine dye molecules are mostly planar with a carbon bridge extended along one direction (x), with a π electron density. However, along the y and z directions at long range, there is no electron density and thus reduced screening in v_W. We note that in real space, it is clear that the CAM-LDA0 and BNL (an optimally tuned long-range exchange functional) are not able to achieve the correct shape nor absolute magnitude of exchange at most length scales, noting especially bad convergence at the short/medium distances. The inadequacy of traditional range-separated hybrids was noted in Ref. 2, which states that "LC-DFT (long-range corrected DFT) is most efficient when discrepancies given by HF and GGA (generalized gradient approximation) evolve with opposite trends. For cyanines, both HF and GGA predict excitation energies that are decreasing much too slowly with chain length."

Figure 3(a) presents results for the Flav-7 dye derivatives, IR-27 and IR-26. We include these dyes as an example where the difference in redshifts is not due to increased binding energy in IR-27, as shown in (b) but is due to a ground-state effect of the LUMO and HOMO energies. This ground-state energy difference is manifested in the difference in HOMO densities near the polymethine bridge due to the electron-withdrawing effect of oxygen (IR-27) vs sulfur (IR-26) (c). Due to how redshifted in energy these dyes are, they serve as another proof that the accuracy of this method does not deteriorate for infrared excitations.

Figure 4 compares the optical gaps for all 13 dyes predicted by various methods with the experimental references

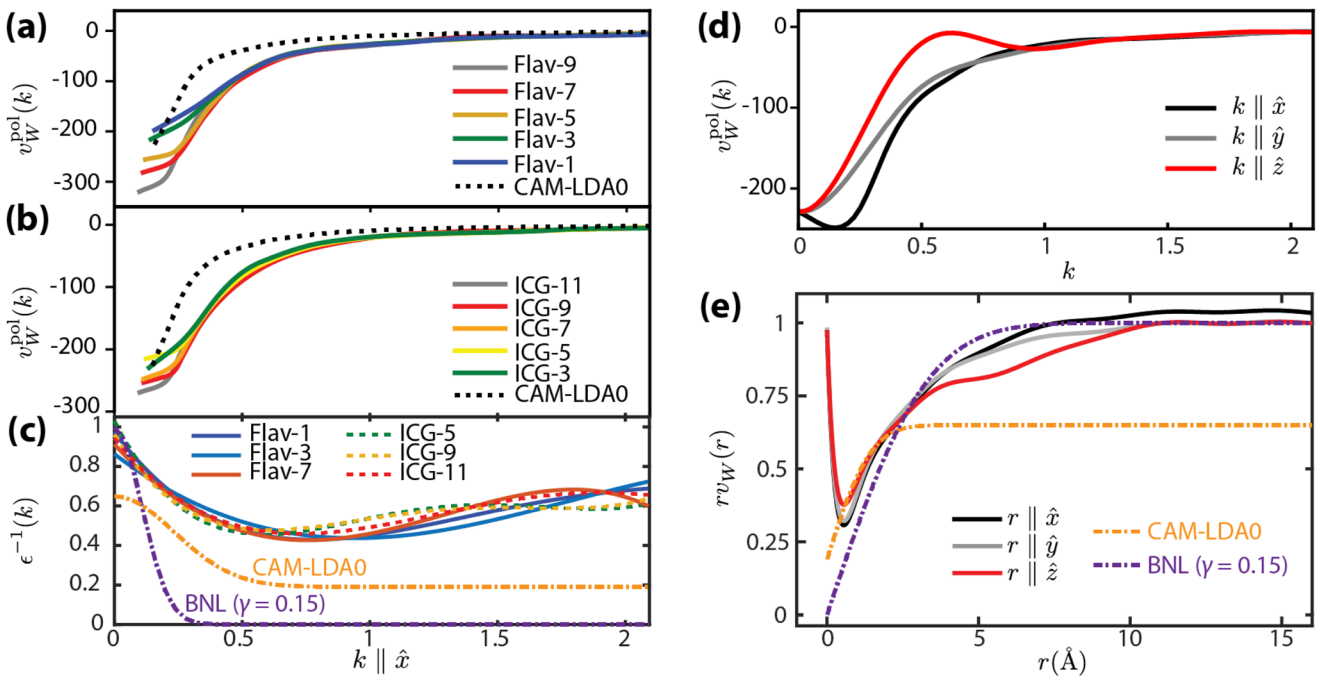

FIG. 2. Plot of individually fitted $v_W(k)$ along the x-axis of the polymethine bridge for the (a) Flav and (b) ICG dye families. All v_W shown are generated by fitting with 2000 stochastic orbitals. (c) Shifted ratio between the fitted $v_W(k)$ and the bare Coulomb potential $v(k) = 4\pi/k^2$, i.e., $\epsilon^{-1}(k) \equiv 1 + k^2 v_W(k)/(4\pi)$. (d) Spatial components of the fitted v_W^{pol} along the cardinal k-paths $(k_x, 0, 0)$, $(0, k_y, 0)$, and $(k_z, 0, 0)$, and the complement in real space (e) showing $rv_W(r)$, an alternative representation of the dielectric screening at varying inter-atomic distances. All variables are in atomic units unless otherwise stated.

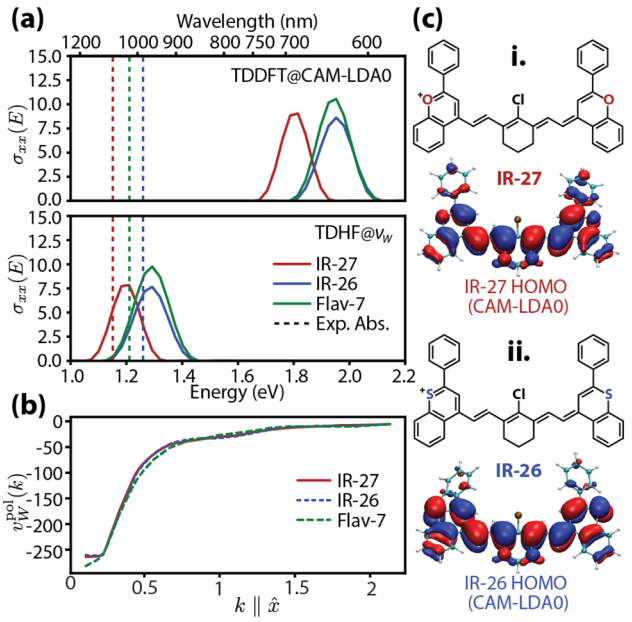

FIG. 3. Spectral results (a) and stochastically fitted v_W interaction (b) for the cyanine dyes IR-27 and IR-26 (c).

(Refs. 11, 13–16, and 26). TDHF@v_W achieves a significantly improved mean absolute error (MAE) of 0.09 eV. In contrast, among all TDDFT functionals, TD-CAM-B3LYP produces an MAE of 0.63 eV; TD-CAM-LDA0 yields 0.66 eV; TD-PBE0 results in 0.79 eV; and TD-local-density approximation (LDA) shows 0.55 eV. The substantial improvement of TDHF@v_W aligns with the enhancements observed with the full deterministic BSE in model dye systems at a significantly reduced computational cost.[2]

Our study has shown the power of a new approach, TDHF@v_W, which fits the full many-body screened-exchange interaction based on the BSE within the TDHF framework.[6,7] This method successfully addresses the longstanding challenge of accurately predicting the optical properties of polymethine dye molecules, surpassing the limitations of traditional TDDFT calculations. Analyzing the fitted polarization potential (v_W^{pol}) and the fraction of exact exchange removed due to screening, we identify similarities across different dye families, suggesting the potential for a universal screened exchange kernel applicable to highly delocalized organic systems. Moreover, our findings highlight the consistency of results obtained with TDHF@v_W across various polymethine bridge lengths and heterocycles, offering insights into the fundamental properties of these molecules. Our study also elucidates ground-state effects on the optical properties of dye molecules, as evidenced by differences in redshifts between certain derivatives, which are what most previous TDDFT studies of cyanine dyes detect. This observation reinforces the robustness of TDHF@v_W in capturing complex electronic interactions and ground-state phenomena, particularly for excitations extending into the SWIR region.

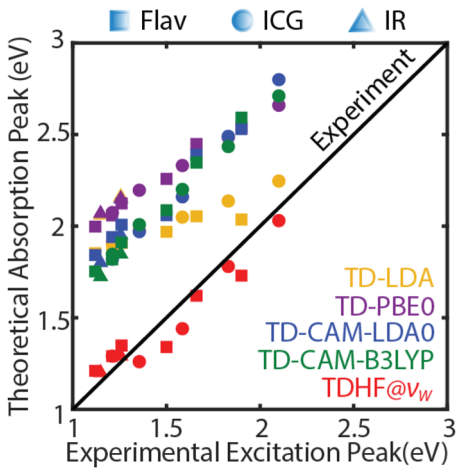

FIG. 4. Optical gaps from various TDDFT functionals and TDHF@v_W against the water solution experimental absorption peaks.

Quantitatively, TDHF@v_W exhibits a substantially reduced MAE compared to traditional TDDFT functionals, indicating its superior accuracy in predicting excitation energies. This improvement, achieved at a manageable computational cost, positions TDHF@v_W as a promising tool for researchers in fields such as biological imaging and materials science, where accurate modeling of optical properties is crucial. In addition, this method realistically scales to bigger sizes, as it is applicable to studying organic chromophores in larger-scale systems, such as biological light-harvesting complexes.

See the supplementary material for geometry optimization procedures, software validation, and stochastic convergence of the methodology.

We extend our gratitude to Anthony Spearman, Quintashia Wilson, and Professor Ellen M. Sletten (UCLA) for their suggestions of polymethine dye molecules. N.C.B. acknowledges the NSF Graduate Research Fellowship Program under Grant No. DGE-2034835. N.C.B. and B.Y.L. acknowledge the computing resources provided by ACCESS allocation Grant Nos. CHE-230099 and CHE-240029, and the Expanse system at the San Diego Supercomputer Center. J.R.C. was supported by NSF Grant No. NSF CHE-2204263. D.N. was supported by NSF Grant No. CHE-2245253. This work also used computational services associated with the Hoffman2 Shared Cluster provided by UCLA Office of Advanced Research Computing's Research Technology Group.

AUTHOR DECLARATIONS

Conflict of Interest

The authors have no conflicts to disclose.

Author Contributions

Nadine C. Bradbury: Conceptualization (lead); Data curation (equal); Formal analysis (equal); Funding acquisition (supporting); Methodology (equal); Software (lead); Validation (equal); Visualization (equal); Writing – original draft (equal); Writing – review & editing (equal). **Barry Y. Li**: Conceptualization (equal); Data

curation (equal); Formal analysis (equal); Investigation (equal); Validation (equal); Visualization (equal); Writing – original draft (equal); Writing – review & editing (equal). **Tucker Allen**: Methodology (equal); Software (equal). **Justin R. Caram**: Investigation (equal); Supervision (equal); Writing – review & editing (equal). **Daniel Neuhauser**: Methodology (lead); Project administration (equal); Software (lead); Supervision (equal); Writing – review & editing (equal).

DATA AVAILABILITY

The data and software that support the findings of this study are available from the corresponding author upon reasonable request.

REFERENCES

[1]H. Kuhn, J. Chem. Phys. **16**, 840–841 (1948).
[2]B. Le Guennic and D. Jacquemin, Acc. Chem. Res. **48**, 530–537 (2015).
[3]D. Jacquemin, E. A. Perpète, G. E. Scuseria, I. Ciofini, and C. Adamo, J. Chem. Theory Comput. **4**, 123–135 (2007).
[4]P. Boulanger, D. Jacquemin, I. Duchemin, and X. Blase, J. Chem. Theory Comput. **10**, 1212–1218 (2014).
[5]D. Jacquemin, I. Duchemin, and X. Blase, J. Phys. Chem. Lett. **8**, 1524–1529 (2017).
[6]N. C. Bradbury, M. Nguyen, J. R. Caram, and D. Neuhauser, J. Chem. Phys. **157**, 031104 (2022).
[7]N. C. Bradbury, T. Allen, M. Nguyen, K. Z. Ibrahim, and D. Neuhauser, J. Chem. Phys. **158**, 154104 (2023).
[8]R. Baer, E. Livshits, and U. Salzner, Annu. Rev. Phys. Chem. **61**, 85–109 (2010).
[9]S. Sharma, J. K. Dewhurst, A. Sanna, and E. K. U. Gross, Phys. Rev. Lett. **107**, 186401 (2011).
[10]J. Zhan, M. Govoni, and G. Galli, J. Chem. Theory Comput. **19**, 5851–5862 (2023).
[11]E. D. Cosco, J. R. Caram, O. T. Bruns, D. Franke, R. A. Day, E. P. Farr, M. G. Bawendi, and E. M. Sletten, Angew. Chem., Int. Ed. **56**, 13126–13129 (2017).
[12]M. A. Mosquera, C. H. Borca, M. A. Ratner, and G. C. Schatz, J. Phys. Chem. A **120**, 1605–1612 (2016).
[13]M. M. Swamy, Y. Murai, K. Monde, S. Tsuboi, A. K. Swamy, and T. Jin, ACS Appl. Mater. Interfaces **16**, 17253 (2024).
[14]H. Langhals, A. Varja, P. Laubichler, M. Kernt, K. Eibl, and C. Haritoglou, J. Med. Chem. **54**, 3903 (2011).
[15]R. S. Gamage and B. D. Smith, Chem. Biomed. Imaging **2**, 384 (2024).
[16]H. Heng, G. Song, X. Cai, J. Sun, K. Du, X. Zhang, X. Wang, F. Feng, and S. Wang, Angew. Chem., Int. Ed. **61**, e202203444 (2022).
[17]N. C. Bradbury, T. Allen, M. Nguyen, and D. Neuhauser, J. Chem. Theory Comput. **19**, 9239–9247 (2023).
[18]M. Sereda, T. Allen, N. C. Bradbury, K. Z. Ibrahim, and D. Neuhauser, J. Chem. Theory Comput. **20**, 4196–4204 (2024).
[19]E. D. Cosco, A. L. Spearman, S. Ramakrishnan, J. G. P. Lingg, M. Saccomano, M. Pengshung, B. A. Arús, K. C. Y. Wong, S. Glasl, V. Ntziachristos, M. Warmer, R. R. McLaughlin, O. T. Bruns, and E. M. Sletten, Nat. Chem. **12**, 1123–1130 (2020).
[20]J. T. Alander, I. Kaartinen, A. Laakso, T. Pätilä, T. Spillmann, V. V. Tuchin, M. Venermo, and P. Välisuo, Int. J. Biomed. Imaging **2012**, 940585 (2012).
[21]F. Neese, "Software update: The ORCA program system—Version 5.0," Wiley Interdiscip. Rev.: Comput. Mol. Sci. **12**, e1606 (2022).
[22]V. Vlček, E. Rabani, and D. Neuhauser, Phys. Rev. Mater. **2**, 030801(R) (2018).
[23]X. Blase, I. Duchemin, D. Jacquemin, and P.-F. Loos, J. Phys. Chem. Lett. **11**, 7371 (2020).
[24]T. Allen, M. Nguyen, and D. Neuhauser, "GW with hybrid functionals for large molecular systems," J. Chem. Phys. **161**, 114116 (2024); arXiv:2405.12306.
[25]C. A. McKeon, S. M. Hamed, F. Bruneval, and J. B. Neaton, J. Chem. Phys. **157**, 074103 (2022).
[26]H. C. Friedman, E. D. Cosco, T. L. Atallah, S. Jia, E. M. Sletten, and J. R. Caram, Chem **7**, 3359 (2021).
[27]D. Neuhauser, J. Chem. Phys. **93**, 2611 (1990).
[28]T. Yanai, D. P. Tew, and N. C. Handy, Chem. Phys. Lett. **393**, 51–57 (2004).
[29]Y. Tawada, T. Tsuneda, S. Yanagisawa, T. Yanai, and K. Hirao, J. Chem. Phys. **120**, 8425–8433 (2004).